This is an *Accepted Manuscript*, which has been through the Royal Society of Chemistry peer review process and has been accepted for publication.

Accepted Manuscripts are published online shortly after acceptance, before technical editing, formatting and proof reading. Using this free service, authors can make their results available to the community, in citable form, before we publish the edited article. We will replace this *Accepted Manuscript* with the edited and formatted *Advance Article* as soon as it is available.

You can find more information about *Accepted Manuscripts* in the **Information for Authors**.

Please note that technical editing may introduce minor changes to the text and/or graphics, which may alter content. The journal's standard **Terms & Conditions** and the **Ethical guidelines** still apply. In no event shall the Royal Society of Chemistry be held responsible for any errors or omissions in this *Accepted Manuscript* or any consequences arising from the use of any information it contains.

Hydrothermal Synthesis as a Route to Mineralogically-Inspired Structures

Colin D. McMillen and Joseph W. Kolis*

Department of Chemistry and Center for Optical Materials Science and Engineering

Technologies (COMSET), Clemson University, Clemson, South Carolina 29634-0973, USA

Corresponding Author Contact:

Joseph W. Kolis
485 H.L. Hunter Laboratories
Clemson, SC 29634
Tel. 864-656-4739
Fax: 864-656-6613
e-mail: kjoseph@clemson.edu

Hydrothermal Synthesis as a Route to Mineralogically-Inspired Structures

Colin D. McMillen and Joseph W. Kolis*

Department of Chemistry and Center for Optical Materials Science and Engineering Technologies (COMSET), Clemson University, Clemson, South Carolina 29634-0973, USA

Abstract

The use of high temperature hydrothermal reactions to prepare crystals having mineralogically-related structures is described. Complex naturally occurring minerals can have fascinating structures and exhibit important features like low dimensionality, noncentrosymmetry, or ion channels that can provide excellent guideposts for the designed synthesis of new materials. Actual minerals, even though they may have intriguing physical properties, are often unsuitable for study because of the persistent impurities inevitably present in natural samples. Hydrothermal fluids at relatively high temperatures provide access to large, high quality single crystals of structures with mineral-like structures. This enables the study of physical properties like ionic conduction, magnetic spin frustration and non-linear optical behavior. Some fundamental considerations of the hydrothermal technique are discussed in the context of synthesizing mineralogically-inspired materials. The metal vanadates provide a surprisingly rich and diversified range of compounds and are selected to illustrate many of the concepts described here. A series of low dimensional mineral analogs featuring isolated units, chains, and layers have been prepared in the laboratory as large single crystals using a high temperature hydrothermal synthetic methods, and their physical properties are under

investigation. The metal silicates are also highlighted as another promising field of exploration, since their hydrothermal synthesis surprisingly lags behind the enormous literature of the natural silicate minerals. The introduction of heteroelements, such as boron to make borosilicates, appears to also open the door to additional new materials. Many of these new materials have direct equivalents in the mineral kingdom, while others have no known analogs but are reminiscent of minerals and can be classified in the same ways. From these initial results there appears to be a very rich vein of synthetic minerals waiting to be unearthed in the laboratory using the high temperature hydrothermal method.

1. Introduction and Scope

The mineral kingdom is replete with a fascinating array of unusual structures that prompt great interest themselves, but also beg the question of what other related structures can be prepared synthetically.[1-9] Many of these minerals possess low dimensional structures such as chains or layers, and if such structures contain open shell metal ions, they can have interesting and useful magnetic properties. They may have structures that lack a center of symmetry or have a polar axis, which could lead to complicated ferroic behavior. They can also possess some of the most complex structures ever discovered.[10] These mineral structures have been entering the scientific database at a steady pace since the development of crystallography, and often possess a beauty that inspires mineralogists but is sometimes overlooked by classical solid-state chemists and physicists. We are by no means the first to postulate this concept and a number of fascinating reviews can be consulted for more information.[11-14] In this paper we attempt to highlight some of

the challenges and opportunities in transferring the chemistry from the mineral kingdom to the laboratory bench.

One limitation to the straightforward transfer of understanding between the two fields is the inherent impurity of natural mineral samples, since they are almost always contaminated with the wide variety of dopants that exist in the natural geological environment. Natural crystal growth in such uncontrolled chemical environments invariably leads to substitution at multiple sites with many different metal ions. While this can sometimes lead to interesting stoichiometric distributions, it more often limits the interpretation of inherent physical properties of the structure. There are many minerals that contain low dimensional structures with open shell d-block transition metals like Cu^{2+} for example, which might display novel magnetic behavior,[15] but great care must be exercised in interpreting data obtained from actual minerals. Interesting data may be due to an exciting new physical phenomenon, or simply due to the fact that the Cu^{2+} sites are heavily substituted by other divalent ions that affect the measurements. Nevertheless, the attractive structures of the minerals can serve as a starting point to design synthetic reactions and to study the physical properties of the resultant products. The data can subsequently be interpreted more confidently with the knowledge that the chemical composition is well known.

The natural minerals can also stimulate thought-provoking exercises in subtle structural understanding. Indeed the solid-state chemists can exploit the insights of the mineralogists, who perhaps have more experience in analyzing in detail the structural relationships among such complex materials. For example, fillowite, with the modest empirical formula of $Na_2CaFe_7(PO_4)_6$, has an exceptionally complicated structure with a unit cell approaching 8800 $Å^3$.[16] The structure, however, has been deconstructed to the point where it is proposed as an analog to the simple structure of elemental iron.[17] Additional questions are raised by a detailed

consideration of the mineral structure palette. Consider the mineral McGovernite, which is found all around the world but whose structure is still largely unknown. It has a "nominal" formula of $Mn_{273}As^{III}_{12}As^{V}_{30}Si_{42}O_{324}(OH)_{252}$, which obviously is only approximate at best, and has a unit cell axis of approximately 204 Å, with possibly up to 1150 unique atoms.[18] Yet it has been isolated from locations ranging from Namibia to New Jersey. If such a bizarre specimen can form in diverse natural environments all over the world, there is certainly no limit to the related structural variations that can be designed and built in the lab.

There is a broad subfield in geochemistry dedicated to the deduction of chemical conditions of mineral origin.[19] The topic of geochemical origin of minerals is a very wide-ranging one and well beyond the purview of this paper. We focus rather on how their possible origins can serve as a general guideline for further exploration in the laboratory. It is known that many of the interesting and complex mineral structures such as phosphates, sulfates, borates, carbonates, and many others are of hydrothermal origin. If we can generally approximate these natural conditions in the laboratory it is reasonable to hope to make not only direct mineral analogs but also many other similar phases. Given the enormous number of beautiful mineral phases, it gives us great encouragement to know that such an array of materials is freely available.

An interesting construct employed by geochemists and mineralogist is the role that mineral evolution plays in the development of observed structures.[19-22] Primary species such as relatively simple oxides are defined as rock forming species, and these interact over time in natural conditions, transforming to more structurally complex species. Often these transformations take place in superheated water under pressure beneath the earth's surface. These so called hydrothermal conditions can range in temperature from 100 to approximately

700 ˚C in a wide variety of solutions. Such a range of temperatures and chemical environments are responsible for much of the wide variety of attractive mineral structures and are also exactly the conditions we can emulate in the laboratory.[23-28] Thus, by exploiting the similarity between natural mineral growth conditions and our laboratory techniques we can explore the structural relationship of extended structures from hydrothermal fluids, using the natural materials as our inspiration.

2. Hydrothermal Experimental Design

2.1 Historical Overview

The initial work on hydrothermal synthesis was specifically designed to study the growth of important minerals and model natural reaction chemistry to access commercially significant materials like $CaCO_3$ and α-quartz. The very earliest attempts at hydrothermal growth were focused on $CaCO_3$ in the late 1800's, but attention quickly turned to the investigation of α-quartz in the early 20th century.[29,30] The initial hydrothermal work on quartz was based on interest in modeling geochemical synthesis, but was also driven by the importance of α-quartz as an acoustic detection material in sonar and wireless communication. It is particularly significant in that there is not really another synthetic route to the desired phase since it undergoes transformation to the β phase at only 573˚C. The development of hydrothermal quartz growth for commercial applications is a fascinating example of technological history and has been recounted a number of times.[31-34] In an article in 1913,[35] Morey and Niggli provided a comprehensive review of the lab-based hydrothermal growth of a wide range of naturally occurring minerals. The breadth of compounds described provided indisputable evidence of the

power of the hydrothermal method as a tool to prepare natural minerals as man-made crystals. In a later review by Morey, he provides considerable detail on hydrothermal experimental technique and makes the case very clearly, stating "It is clear that the author and his co-workers are trying to reproduce a liquid similar to the magma from which minerals crystalize in nature."[36]

By the late 1950's the hydrothermal synthesis of α-quartz entered the marketplace as a commercial process, and by the mid 1960's the process was essentially fully optimized. By the mid 1970's there were a few groups, mostly in industrial and government laboratory settings, employing hydrothermal synthesis to investigate a number of other systems including zeolites,[37,38] $AlPO_4$,[39] and $KTiO(PO_4)$ (KTP).[40,41] In the late 1980's and early 1990's Haushalter and coworkers began an extensive program on the hydrothermal exploration of reduced metal phosphates.[42-45] This work represents one of the earliest modern examples of original exploratory hydrothermal chemistry. Among other things, they highlighted the beauty and complexity lurking in the phosphate mineral kingdom. Phosphate minerals with convoluted structures like cacoxinite [46] and betpakdalite [47] were underscored as relatives to the synthetic metal phosphates. These curiosities were known to the structural mineralogists, but solid-state chemists were generally not well acquainted with them until this time. Another important point well-made by Haushalter at the time is the importance of graphical display in visualizing the structural features.[45] Often these materials display extreme structural complexity, and the ability to visualize key features is vital to understanding and appreciating their character. The elegant analysis and advanced graphics employed by this group did much to highlight the relationship between lab-grown crown crystals and complex natural minerals.

2.2 Synthetic Approach

At this point we should highlight a distinction in the hydrothermal method, driven purely by experimental factors. In the strictest sense, hydrothermal solvents are any aqueous phases above the boiling point of water. Obviously to prevent the simple boiling off of the solvent, it must be contained under pressure that is greater than atmospheric, usually in an autoclave.[23] The well-known commercially available metal autoclaves ("digestion vessels") lined with inert fluoropolymers are safe, simple and convenient to use, and can easily contain solutions that are acidic, basic or strongly oxidizing. The primary limitation to these autoclaves is the thermal response of the fluoropolymer. Despite many attempts to address this issue, the liners are generally limited to 240°C, while above this temperature the polymer flows and the containers leak. For exploratory investigation of phase space below 240°C, these are quite suitable, leading to rapid examination of new compounds. For many systems this experimental design is sufficient for the growth of pure powders or small single crystal suitable for structure determination by single crystal X-ray diffraction. To a large degree this technology played a major role in the rapid explosion of the metal organic frameworks (MOF) field, which is now ubiquitous in many areas of technology.[48]

Unfortunately however, the low temperature technique is not particularly well suited for designed growth of large single crystals, nor is it suitable for refractory metal oxides, which generally require higher synthesis temperatures (400-700°C). At these higher temperatures, containment of water with a density sufficient to perform chemistry and crystal growth (generally 0.60-0.75 g/cm^3) requires the autoclave to be able to withstand an internal pressure of 1-3 kbar (1.5-4.5 kpsi; 100-300 MPa) (Figure 1).[49] The higher temperature fluids are extremely reactive, so they also require inert metal liners (typically silver, gold or platinum) that are welded

completely closed.[50] The high pressures and temperatures require structurally robust autoclaves made of stainless steel or, preferably, nickel-based alloys (Inconel 718 or similar) to contain the pressures.[23,27,28,51,52] The literature is replete with a variety of designs of such autoclaves but most are custom designs and there are really no stock items commercially available at present. It is generally up to the individual investigators to generate their own experimental technology. Once the effort is made to develop suitable experimental designs however, the higher temperature reactions often provide a very rich chemistry with a high "hit rate" of high quality single crystals per reaction. By coincidence the thermal regime around 250°C also represents an important crossover regarding the stability of coordinated water in solid lattices. Above this temperature, hydrated species are considerably less stable with respect to more condensed solids like hydroxides and oxides, which thus typically require higher temperature hydrothermal fluids for their synthesis and crystal growth.

Figure 1: Technology in hydrothermal synthesis (from left): stainless steel acid digestion vessel with PTFE liner (Parr Instrument Co.), Inconel 718 Tuttle cold-seal autoclave with silver reaction ampoules, scalable to larger sizes.

The hydrothermal method is particularly well suited for amphoteric oxides (i.e. those that have both mild acidic and basic characteristics). Silicates, aluminates, borates, phosphates and related oxides generally display a very rich hydrothermal chemistry and can form an extensive array of structures by coordinating to alkali/alkaline earth ions, first row d-block transition metal ions and lanthanide ions. It is no coincidence that these amphoteric oxides also have the most extensive mineralogical chemistry as well. We typically try to emulate the mineralogical conditions by performing our hydrothermal reactions over the temperature range of 550-650 °C. The reactions themselves occur in sealed precious metal ampoules to contain the corrosive mineralizer solutions. The ampoules are contained within an autoclave filled with a suitable amount of water to provide a positive counter-pressure, usually around 20-30 kpsi (140-210 MPa). Typical synthesis reactions proceed for 3-7 days. The technique is simple and inexpensive and amenable to large numbers of exploratory reactions. The primary limitation is that the inexpensive silver ampoules cannot be used for acidic or oxidizing environments, and the much more expensive gold or platinum liners are required for those reactions. In all cases the metal from the used ampoules is easily recycled. An additional limitation of this technique is the inability to probe the soluble intermediates or obtain any other significant details about the reaction process. Thus any specific mechanistic information would be speculative at best, even for the most well-studied reactions.

Our target structural model involves a scheme familiar to both mineralogists and traditional solid-state chemists, which is the combination of octahedral and tetrahedral building blocks. For example, the octahedra formed by common first row d-block elements (Fe, Mn, Cu, Co Cu etc.), can be combined with tetrahedral anions $(XO_4)^{2-}$ (X = S, Mo, W), $(YO_4)^{3-}$ (Y = P, As, V), $(SiO_4)^{4-}$ and $(ZO_4)^{5-}$ (Z = B, Al) to generate a huge variety of new structures.[1-3,10] Since most

of these transition metal ions and the tetrahedral building blocks are also ubiquitous in natural systems, conditions are ripe for a high degree of overlap between the natural and man made materials. Since the first row d-block metal ions also tend to have interesting magnetic and spectroscopic properties, they make for intriguing targets for laboratory synthetic study. In these systems the products are not necessarily the thermodynamically stable species since they are prepared at an intermediate temperature (400-700˚C) versus the much higher temperature regime of melt-based or flux synthesis. Thus the products may vary considerably from those observed in traditional phase diagrams for example.

The phosphates are an attractive starting point because they represent a common naturally occurring tetrahedral building block. The structural mineralogists seem to have a mixed relationship with the phosphate minerals. On one hand they are pleased by the structural variety among the phosphates, but on the other they seem somewhat disconcerted by the complexity and seemingly arbitrary nature of their chemistry.[53] The phosphates themselves rarely form polymeric species in these environments, and usually occur as isolated tetrahedra or, less often, as the $[P_2O_7]^{4-}$ pyrophosphate group. However, $[PO_4]^{3-}$ does adopt just about every possible chelating and bridging environment imaginable, which leads to a huge variety of structural possibilities. It is clear that the hydrothermal method is an excellent route to new metal phosphates, some of which are new structural types while others are direct mineral analogs. Extension of these concepts to other oxyanion building blocks introduces a wealth of new possibilities, and led us to start thinking more deeply about the relationship between natural and synthetic systems.

3. Mineralogically-inspired Hydrothermal Synthesis

3.1 Vanadates

A specific interest to us is the vanadate unit. Vanadates are isoelectronic with the phosphates and arsenates, and can form similar structures.[54] However, there can also be structural and electronic differences, and in particular vanadates can exhibit significant differences in magnetic coupling effects because of the presence of d-orbitals in the bridging groups.[55] We were originally motivated by our interest in rare earth vanadates, like YVO_4, for optical applications.[56-59] Some interesting descriptive chemistry encountered in those early studies led us to extend our investigations to other metal vanadates. This chemistry has proven to be exceptionally rich and we were able to isolate an array of new metal vanadates that are analogous to, or have close relationships with mineral species. One classification scheme for describing such compounds is through the degree of dimensionality of the crystal structures.[1,2,20] In particular this is useful since low dimensionality often leads to interesting magnetic, electronic, or ferroic behavior. As a guiding principle, the greater the ratio of alkali and alkaline earth metal ions present, the lower the dimensionality. These metal ions retain much of their ionic character and serve to break up the linkages of the oxygen atoms of the bridging groups.
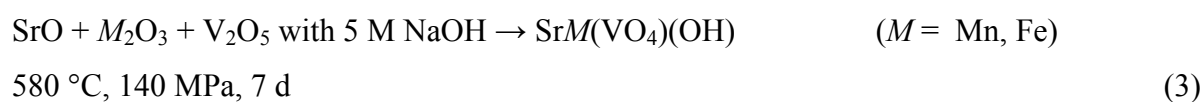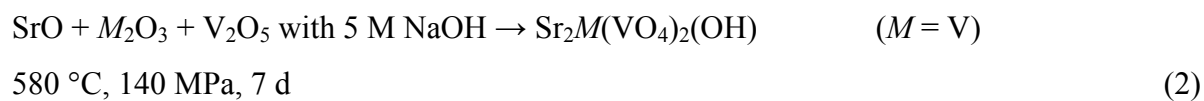
A starting point for us in the vanadate series is the simple hydrothermal reaction 1.[60]

$$BaO + M_2O_3 + V_2O_5 \text{ in 5 M NaOH} \rightarrow Ba_2M(VO_4)_2(OH) \qquad (M = V, Mn, Fe)$$
$$650 \text{ °C, 150 MPa, 10 d} \tag{1}$$

The product of this reaction resembles minerals of the brackebuschite family, $Pb_2(Mn,Fe)(VO_4)_2(OH)$.[61,62] The dominant features of this structure type are the isolated one-dimensional transition metal chains (Figure 2a). The chains propagate along the *b*-axis through shared oxygen edges of the transition metal octahedra. The hydroxide group in the formula also

participates in this bridging. The vanadate groups bridge between neighboring transition metal octahedra along the length of the chains, but do not crosslink between neighboring chains. Thus the one-dimensional vanadate-decorated chains are isolated from one another by Ba^{2+} ions. Transition metal interactions in such isolated edge-sharing one-dimensional chains often lead to interesting magnetic behavior. Indeed, our initial magnetic studies on the S =1 system of the V^{3+} analog indicate spin-gap behavior above 30 K that warrants further study.[60] The large size of the pure crystals obtained (2-3 mm in size) from reactions at 650 °C enables more detailed characterization of these samples. For example, the pronounced Jahn-Teller distortion about Mn^{3+} in $Ba_2Mn(VO_4)_2(OH)$ was also detected from the structural study, where Mn-O bonds range from 1.930(3) to 2.191(3) Å. The extent of the effect in this structure type was previously unclear based on the structural analysis of natural brackebuschite due to mixing of Jahn-Teller inactive Fe^{3+} ions with Mn^{3+} at the transition metal site (M-O bonds ranging from 1.98(2) to 2.10(2) Å).[60]

A minor modification of reaction 1, where Sr^{2+} is substituted for Ba^{2+}, proved to be less straightforward than expected (2, 3).[63]

$SrO + M_2O_3 + V_2O_5$ with 5 M NaOH $\rightarrow Sr_2M(VO_4)_2(OH)$ ($M = V$)
580 °C, 140 MPa, 7 d   (2)
$SrO + M_2O_3 + V_2O_5$ with 5 M NaOH $\rightarrow SrM(VO_4)(OH)$ ($M = $ Mn, Fe)
580 °C, 140 MPa, 7 d   (3)

These reactions exhibited sensitivity to the transition metal identity, producing a brackebuschite derivative in the case of vanadium, and descloizite ($Pb(Zn,Cu)(VO_4)(OH)$) derivatives in the cases of Mn and Fe, whereby we observe reduction of the transition metals to divalent oxidation states with formation of the descloizite-type structure.[64] This structure type features similar

vanadate-decorated one-dimensional edge sharing transition metal chains, but in this case the chains do crosslink with one another via the VO_4 tetrahedra (Figure 2b). This may be due in part to the stoichiometry of the material's lower relative ratio of the alkaline earth metal to transition metal (1:1) compared to brackebuschite (2:1). In the descloizite-type $SrM(VO_4)(OH)$ the oxygen atoms of the VO_4 groups satisfy their valence by bridging the neighboring transition metal chains instead of to an additional alkaline earth ion as in the brackebuschite structure type. While the structure then becomes somewhat more complex, the construct of the low-dimensional transition metal chains remains intact. Preliminary investigations into the resulting magnetic properties again indicates spin-gap behavior above 30 K for $SrMn(VO_4)(OH)$, with additional long range ordering occurring below 30 K. Multi-millimeter size crystals were again obtained, enabling physical property measurement like single crystal magnetic and neutron diffraction studies for example.
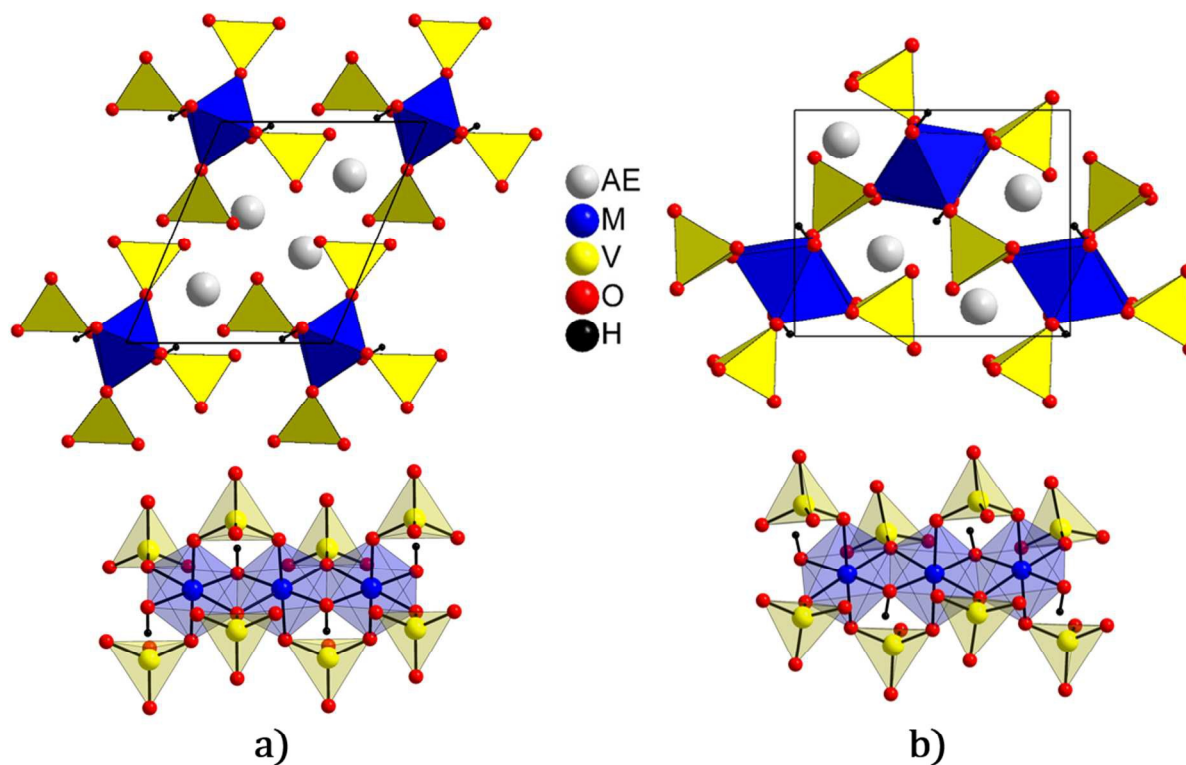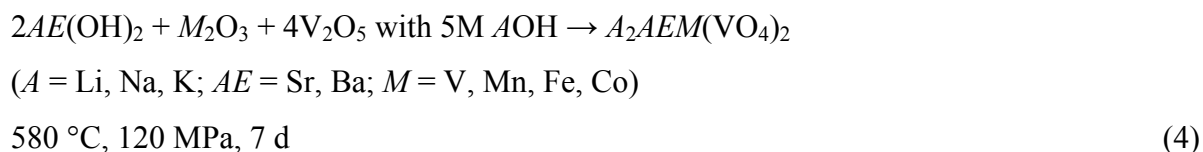

a)   b)

Figure 2: Comparison of brackebuschite ($AE_2M(VO_4)_2(OH)_2$, AE = Ba, M = V, Mn, Fe) and descloizite ($AEM(VO_4)(OH)$, AE = Sr, M = Mn, Co) structure types: a) brackebuschite-type vanadate structure with isolated edge-sharing transition metal chains propagating along [010]; b) descloizite-type vanadate structure with vanadate-bridged edge-sharing transition metal chains propagating along [100]. Representative structural examples are: $Ba_2V(VO_4)_2(OH)$ in space group $P2_1/m$, with a = 7.8783(16) Å, b = 6.1369(12) Å, c = 9.1836(18) Å, β = 113.07(3) °, Z = 2,[60] and $SrMn(VO_4)(OH)$ in space group $P2_12_12_1$, with a = 6.1322(13) Å, b = 7.7201(19) Å, c = 9.414(2) Å, Z = 4.[63]

Slight modification of the reaction stoichiometry (4) leads to different chemistry again.[65]

$2AE(OH)_2 + M_2O_3 + 4V_2O_5$ with 5M $AOH \rightarrow A_2AEM(VO_4)_2$

(A = Li, Na, K; AE = Sr, Ba; M = V, Mn, Fe, Co)

580 °C, 120 MPa, 7 d   (4)

These materials are members of the glaserite class, $K_3Na(SO_4)_2$.[66,67] More generally, the glaserite formula can be described as $A_2A'B(TO_4)_2$ with the variety of unique sites leading to numerous combinations of formulae, classifying it as a highly adaptable structure.[68] The vanadate glaserites here (T = V^{5+}), contain an alkali metal at the A site, an alkaline earth metal at the A' site, and a divalent transition metal at the octahedral B site. Previously, we also isolated a series of glaserites where the A and A' sites are both occupied by K^+ ions, and the B site is occupied by a trivalent rare earth ion with the general formula of $K_3RE(VO_4)_2$, (RE = Sc, Y, Lu-Dy). These compounds form as fairly large single crystals (2-5 mm) and exhibit interesting optical properties, as well as potentially interesting magnetic properties.[69]

The glaserite structure is a departure from the brackebuschite-type and descloizite-type vanadates described above. Here, the transition metal octahedra are completely isolated from one another by the surrounding vanadate tetrahedra (Figure 3). This arrangement creates metal vanadate sheets in the ab plane, which alternate with layers of alkali and alkaline earth metals

15

along the c-axis. Again, the higher ratio of alkali and alkaline earth metals to the transition metals in glaserites (3:1) compared to the descloizite system (1:1) appears to prevent cross-linking of the sheets by the vanadates. The series also presents an interesting study in some of the structural distortions in the glaserite structure.[65] For example, the $A_2BaM(VO_4)_2$ phases with Na^+ and K^+ at the A site crystallize in the ideal glaserite structure in space group *P-3m1*. This is a rather high symmetry system where the divalent transition metal possesses -3m symmetry and the vanadium site possesses 3m symmetry. (Figure 3a). When the smaller Li^+ occupies the A site the symmetry is lowered to space group *P-3*. This introduces a rotation of the transition metal vanadate layers (Figure 3b) to bring the oxygen atoms into a position to coordinate the Li atoms. Modification of the A' site from Ba^{2+} to Sr^{2+} also leads to a further structural distortion, this time into the monoclinic space group *P2₁/c*. This lower-symmetry glaserite also has a direct mineral analog called merwinite $(Ca_3Mg(SiO_4)_2)$.[70] In this case there are two unique transition metal vanadate layers that are rotated relative to one another (Figure 3c). Even in these lower symmetry modifications approximate three-fold symmetry is retained, so the transition metal ions can exist in a magnetically frustrated state.[71]
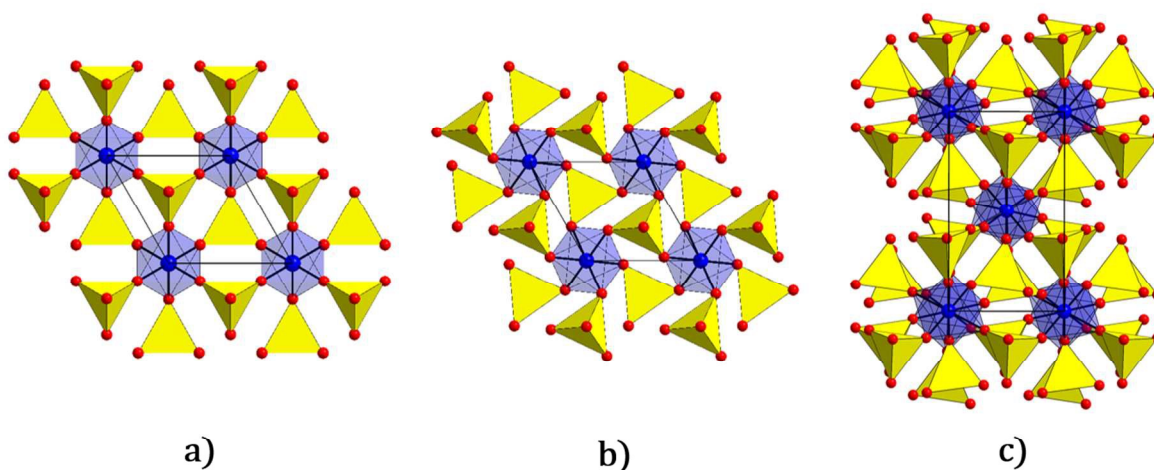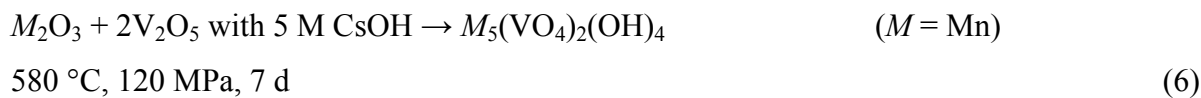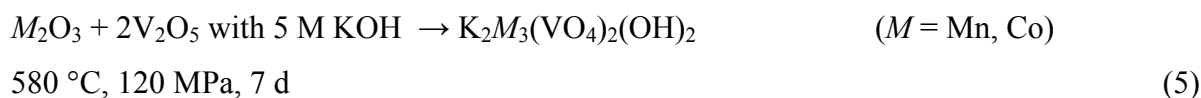

a)   b)   c)

16

Figure 3: Transition metal vanadate layers in the glaserite-merwinite structure type: a) ideal glaserite symmetry in *P-3m1*; b) distorted glaserite symmetry in *P-3*; c) distorted glaserite/merwinite symmetry in *P2$_1$/c*. Representative structural examples are: $K_2BaMn(VO_4)_2$ in space group *P-3m1*, with a = 5.7340(8) Å, c = 7.3859(15) Å, Z = 1, $Li_2BaMn(VO_4)_2$ in space group *P-3*, with a = 5.2887(7) Å, c = 7.3026(15) Å, Z = 1, and $Na_2SrMn(VO_4)_2$ in space group *P2$_1$/c*, with a = 13.823(3) Å, b = 5.5671(11) Å, c = 9.6686(19) Å, β = 90.09(3) °, Z = 4.[65]

With still further variation of the reaction conditions, the alkaline earth component can be removed from the reaction to reveal still more new chemistry.[72]

$$M_2O_3 + 2V_2O_5 \text{ with 5 M KOH } \rightarrow K_2M_3(VO_4)_2(OH)_2 \qquad\qquad (M = Mn, Co)$$

580 °C, 120 MPa, 7 d   (5)

$$M_2O_3 + 2V_2O_5 \text{ with 5 M CsOH} \rightarrow M_5(VO_4)_2(OH)_4 \qquad\qquad (M = Mn)$$

580 °C, 120 MPa, 7 d   (6)

The primary structural feature of $K_2Mn_3(VO_4)_2(OH)_2$ is a two-dimensional sheet of edge-sharing MnO_6 octahedra in the *bc* plane.[73] The sheet is decorated by the vanadate tetrahedra, but due to the presence of the K^+ ions the vanadates do not connect neighboring sheets (Figure 4a, top). The result is a layered structure with alternating transition metal vanadate layers and potassium layers along the *a*-axis. At present, this particular compound has no known mineral analog, but it is similar in many ways to compounds in the series and is isolated from the same types of synthetic reactions. Thus the concept of mineralogically-inspired crystal growth should be considered to extend beyond those compounds having direct mineralogical analogs.

The product of reaction 6, $Mn_5(VO_4)_2(OH)_4$, is a stoichiometric form of the mineral reppiaite, $Mn_{5.01}[(V_{1.65}As_{0.35})O_{8.02}](OH)_{3.98}$.[74] In this reaction, the larger Cs^+ ion is not included in the lattice, and remains in solution. The relatively simple formula, however, belies a very complex structure. In reppiaite we again observe a two-dimensional transition metal sheet structure (in the *bc* plane) with vanadate tetrahedra sharing oxygen corners with the transition

metals. However, with no alkali metal to act as a spacer between layers, the vanadate groups link directly to the next transition metal sheet along the *a*-axis. This creates an overall framework structure containing the low dimensional sheet feature (Figure 4b, top). Differences in the Mn:V ratio in $K_2Mn_3(VO_4)_2(OH)_2$ and $Mn_5(VO_4)_2(OH)_4$ also lead to differences in the nature of the two dimensional manganese oxide sheets. In $K_2Mn_3(VO_4)_2(OH)_2$, manganese atoms form alternating layers of honeycomb and triangular arrangements within the sheets (Figure 4a, bottom). In $Mn_5(VO_4)_2(OH)_4$, layers of Mn atoms form a honeycomb arrangement that alternates with triple layers of triangular Mn atoms to form the two dimensional sheets (Figure 4b, bottom).
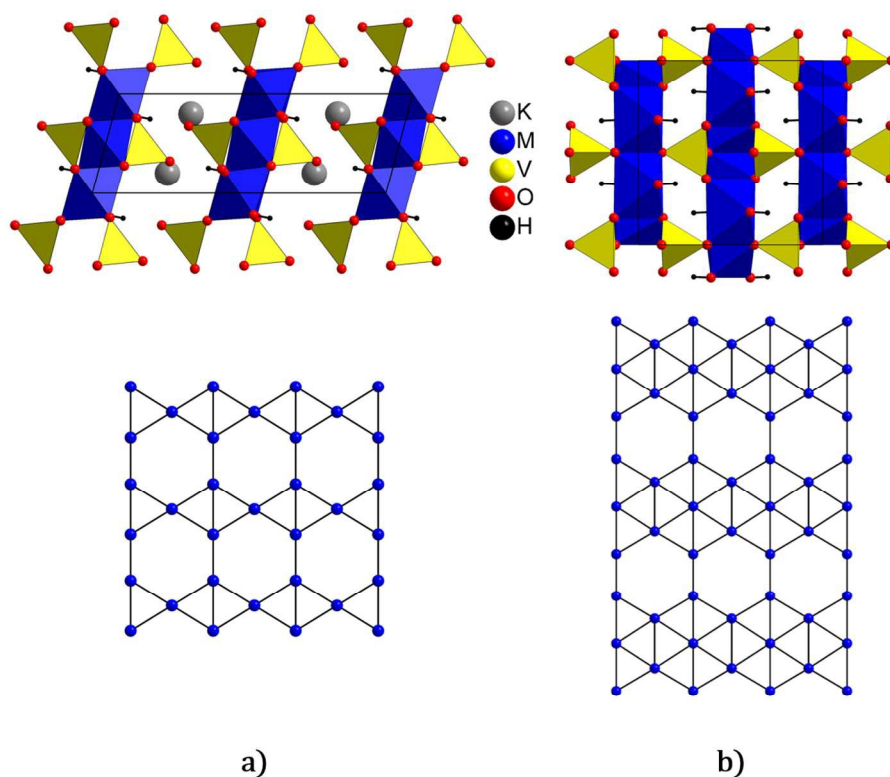

a)   b)

Figure 4: Comparison of a) $K_3M_2(VO_4)_2(OH)_2$ (M = Mn, Co) and b) $M_5(VO_4)_2(OH)_4$ (M = Mn) (reppiaite-type) structures. Top images highlight differences in vanadate connectivity of the transition metal sheets – oriented along [010] for a) and [001] for b). Bottom images highlight the differences in the nature of the transition metal sheets – oriented along [100] for a) and [100] for b). Connections shown between transition metal centers represent shared oxygen edges.

Representative structural examples are: $K_3Mn_2(VO_4)_2(OH)_2$ in space group *C2/m*, with *a* = 15.184(3) Å, *b* = 6.1578(12) Å, *c* = 5.3916(11) Å, β = 105.33(3) °, Z = 2, and $Mn_5(VO_4)_2(OH)_4$ in space group *C2/m*, with *a* = 9.6568(19) Å, *b* = 9.5627(19) Å, *c* = 5.4139(10) Å, β = 98.53(3) °, Z = 2.[72]

As a final example, the reppiaite reaction (6) was modified to use a mixed CsOH/CsF mineralizer solution.[75]

$Cs_2CO_3 + M_2O_3 + V_2O_5$ with 1 M CsOH/6 M CsF $\rightarrow Cs_2M_2(V_2O_7)F_2$ (M = Mn)
580 °C, 120 MPa, 7 d   (7)

The resulting product again has no direct mineralogical analog, but hints at a rich field of new synthetic and structural chemistry that encourages further exploration, as fluorine atoms are now observed in the reaction product. Furthermore, Cs is now included in the structure suggesting that the mineralizer can be useful in building structural complexity back into the system. The, $Cs_2Mn_2(V_2O_7)F_2$ product also demonstrates that polyvanadate oxyanions can be prepared from hydrothermal systems, and V^{5+} is not limited to isolated tetrahedra.

Interestingly, the structure of $Cs_2Mn_2(V_2O_7)F_2$ comes somewhat full-circle in our present discussion of vanadates, as the low dimensional transition metal feature here is an edge-sharing one-dimensional chain (Figure 5). The shared edges consist of one oxygen atom and one fluorine atom, and the chains propagate in a zigzag fashion along the c-axis. In this case, the larger V_2O_7 group enables crosslinking between three chains. The 1:1 ratio of Cs and Mn in this product is again perhaps a director of the cross-linked low-dimensional features, as was observed in the descloizite-type $SrMn(VO_4)(OH)$. The resulting transition metal vanadate framework in $Cs_2Mn_2(V_2O_7)F_2$ creates small channels along the c-axis which contain the Cs^+ cations. Work is

19

underway to characterize the magnetic properties of this chain arrangement, and of course to explore more variations of these thematic reactions.
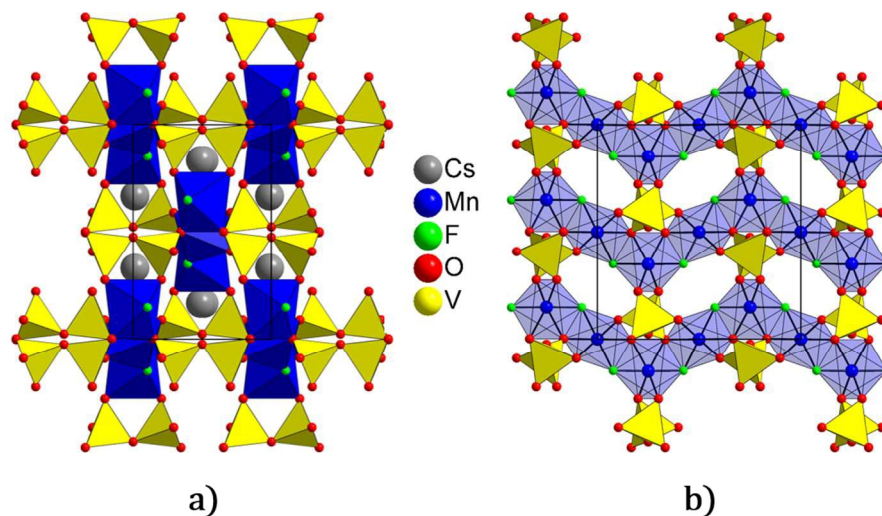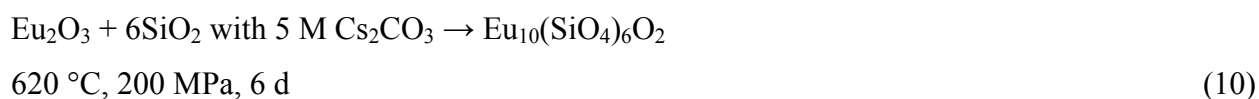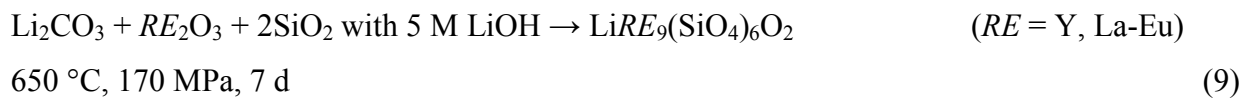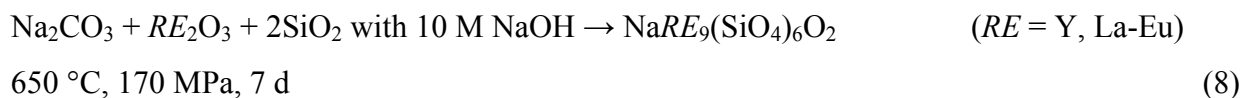

Figure 5: One-dimensional edge-sharing transition metal chains connected by V_2O_7 groups in $Cs_2Mn_2(V_2O_7)F_2$: a) along [001]; b) along [100] (Cs atoms omitted from b) for clarity). Structural details are: $Cs_2Mn_2(V_2O_7)F_2$ in space group *Pbcn*, with *a* = 7.5615(14) Å, *b* = 11.745(2) Å, *c* = 11.127(2) Å, Z = 4.[75]

3.2 Rare Earth Silicates

The next logical step from phosphates and vanadates is the silicates, which are of course the largest and most common of mineralogical categories. In contrast to the phosphates, the silicates readily form many polymeric units as building blocks, along with the monomers and dimers. Surprisingly the synthetic hydrothermal chemistry of the metal silicates is not as well developed as might be expected given their extensive mineral chemistry. Silicates generally require somewhat more robust hydrothermal synthesis conditions compared to phosphates, namely stronger concentrations of mineralizer (typically OH⁻) and higher temperatures (500-

650˚C) to enable the growth of large single crystals. These more rigorous conditions may account for their less extensive hydrothermal synthetic study. Even so, there appears to be a huge number of silicates awaiting discovery by synthesis at temperatures above 400-500˚C. Under such conditions we already encountered interesting chemistry producing derivatives of the wadeite ($Rb_2ThSi_3O_9$) and fresnoite ($Ba_2VSi_2O_8$) families, for example.[76,77]

One straightforward analog between the phosphates to the silicates is the class of compounds called apatites. There is a wide range of phosphate apatites derived from the parent $Ca_{10}(PO_4)_6X_2$, or $Ca_5(PO_4)_3X$ (X = OH, F, Cl).[78] As another highly adaptable structure, the apatites provide numerous means of obtaining charge-balanced species. Consider the following reactions producing silicate oxyapatites.[79]

$Na_2CO_3 + RE_2O_3 + 2SiO_2$ with 10 M NaOH → $NaRE_9(SiO_4)_6O_2$ (RE = Y, La-Eu)
650 °C, 170 MPa, 7 d   (8)
$Li_2CO_3 + RE_2O_3 + 2SiO_2$ with 5 M LiOH → $LiRE_9(SiO_4)_6O_2$ (RE = Y, La-Eu)
650 °C, 170 MPa, 7 d   (9)
$Eu_2O_3 + 6SiO_2$ with 5 M Cs_2CO_3 → $Eu_{10}(SiO_4)_6O_2$
620 °C, 200 MPa, 6 d   (10)

Complete rare earth replacement for calcium in the parent would result in a net +2 charge imbalance in a silicate oxyapatite, but substitutional disorder between Li^+/Na^+ and RE^{3+} at one of the cation sites (Figure 6a) brings the oxyapatite into a charge balanced state as $ARE_9(SiO_4)_6O_2$ (A = Li, Na). Such manipulations can be an important tool for the materials chemist, as the presence of the rare earth site in the silicate oxyapatite permits straightforward doping of optically active rare earth ions into the apatite lattice, enabling the synthesis of new phosphors and optical materials. Rare earths having a stable lower oxidation state provide an alternate path,

as in the case of hydrothermally synthesized $Eu_{10}(SiO_4)_6O_2$ which is reconciled as

$Eu^{II}_2Eu^{III}_8(SiO_4)_6O_2$.[79]

      Simply extending this reaction to the smaller lanthanide ions introduces a significant shift

in the structural chemistry. The small rare earth ions lead to high yields of single crystals of the

formula $ARESiO_4$.[80]

$A_2CO_3 + RE_2O_3 + 2SiO_2$ with 10 M AOH $\rightarrow ARESiO_4$ (A = Li, Na; RE = Y, Dy-Lu)

650 °C, 170 MPa, 7 d   (11)

Interestingly, this "new" synthetic product is structurally analogous to the well-known olivine

mineral family, $(Mg,Fe)_2SiO_4$.[81] $ARESiO_4$ crystals of 2-3 mm in size have been obtained from

simple growth experiments in our labs. It should be noted that that the structures of the LiRESiO$_4$

family are still not yet well understood despite their potential for interesting optical behavior and

promising ionic conductivity.[82] This modified olivine structure features two-dimensional sheets

of corner sharing rare earth octahedra in the bc plane that are connected via isolated silicate

tetrahedra to form the overall framework (Figure 6b). This is similar behavior to what was

observed in the vanadate systems, where a 1:1 ratio of alkali or alkaline earth metal to transition

metal permitted crosslinking of low dimensional features. The olivine-type metal silicate

framework possesses intersecting channels along the b- and c-axes that contain the alkali metals.

These structural features are not always apparent when considering olivine end members such as

forsterite (Mg_2SiO_4) or fayalite (Fe_2SiO_4) or their disordered analogs, since the same atom type

(albeit unique atoms of the same type) occupies both the comparable alkali metal and rare earth

sites in $ARESiO_4$. This gives the appearance of a structure with silicate tetrahedra fitting in

between a highly condensed framework of Mg or Fe atoms. Thus the constructs of low

dimensional layers, or channels permitting ionic conductivity, that can be seen in the mineralogically-inspired species can be overlooked without the synthetic perspective.
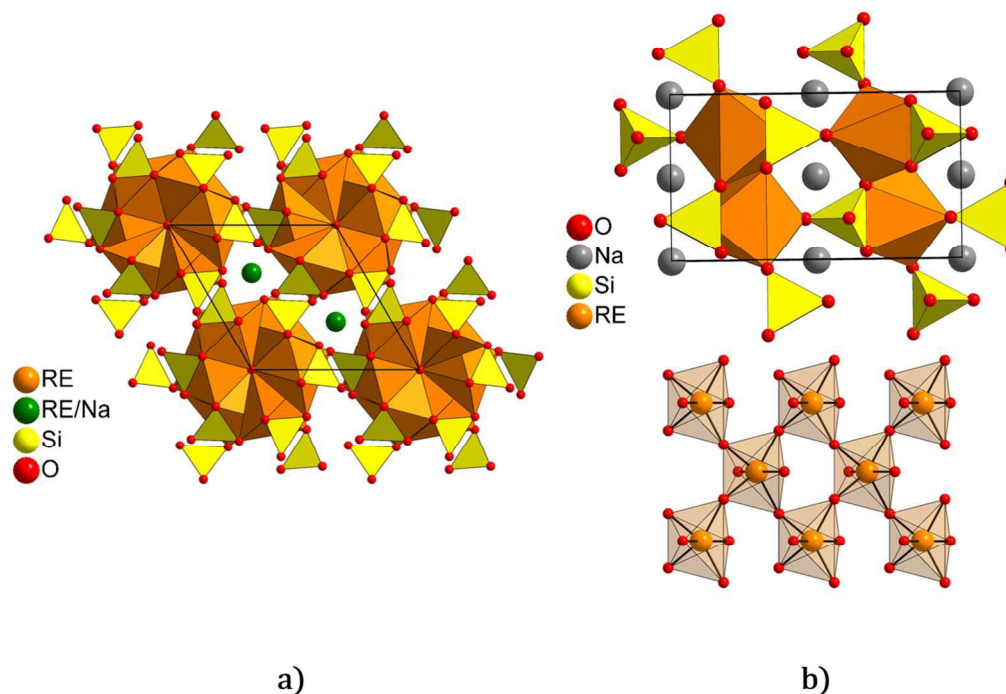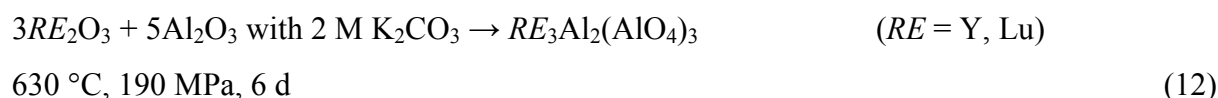

a)   b)

Figure 6: Structures of a) silicate oxyapatite compounds, $NaRE_9(SiO_4)_6O_2$ along [001], and b) olivine-type alkali rare earth silicates, $NaRESiO_4$, top: along [001], bottom: a single corner sharing two-dimensional rare earth sheet along [100]. Representative structural examples are: $NaEu_9(SiO_4)_6O_2$ in space group $P6_3/m$, with a = 9.4413(13) Å, c = 6.9087(14) Å, Z = 1,[79] and $NaLuSiO_4$ in space group $Pnma$, with a = 11.047(2) Å, b = 6.3308(13) Å, c = 5.1180(10) Å, Z = 4.[80]

Another interesting line of mineral-related products from hydrothermal reactions are the garnets. The garnet family is based on eight-coordinate, six-coordinate and four-coordinate building blocks, giving rise to a wealth of crystal chemistry.[83,84] Naturally-occurring garnets tend to be silicate based, such as grossular ($Ca_3Al_2(SiO_4)_3$), andradite ($Ca_3Fe_2(SiO_4)_3$), almandine ($Fe_3Al_2(SiO_4)_3$), and pyrope ($Mg_3Al_2(SiO_4)_3$), among many. The synthetic garnets are an expansive class of well-known materials, widely used on commercial scales as laser materials,

and heavily studied for their optical properties including phosphor, scintillator, and Faraday rotator applications. These synthetic garnets are most often aluminate or gallate derivatives of the natural silicates. We have given particular attention to the aluminate garnets YAG $(Y_3Al_2(AlO_4)_3)$ and LuAG $(Lu_3Al_2(AlO_4)_3)$ that form readily from stoichiometric hydrothermal reactions.[85,86]

$$3RE_2O_3 + 5Al_2O_3 \text{ with } 2 \text{ M } K_2CO_3 \rightarrow RE_3Al_2(AlO_4)_3 \qquad (RE = \text{Y, Lu})$$
$$630 \text{ °C, } 190 \text{ MPa, } 6 \text{ d} \qquad\qquad (12)$$

In these systems our attention is focused not necessarily on establishing new chemistry, but on using the hydrothermal medium to accomplish designed crystal growth (Figure 7). The chemical control of the hydrothermal system for customized doping, and the ability to grow layers of new material on numerous substrate forms provides a unique approach to the concept of the multifunctional single crystal. This includes crystals with multiple zones of dopants, gradients of dopant concentration, customized internal dopant patterning, and single crystal geometries including end-capping, waveguiding, or cladding. Growth is achieved on a seed crystal substrate by establishing a thermal gradient across the autoclave, which separates the reaction into dissolution and growth zones. The solubility difference established by the thermal gradient allows a saturated solution of the feedstock solute to become supersaturated after convective transport to the growth zone where new garnet material is deposited on the substrate. This area is very much in its developmental stages, but the growth of candidate crystals for applications such as self Q-switching and suppression of amplified spontaneous emission has been proven in concept.
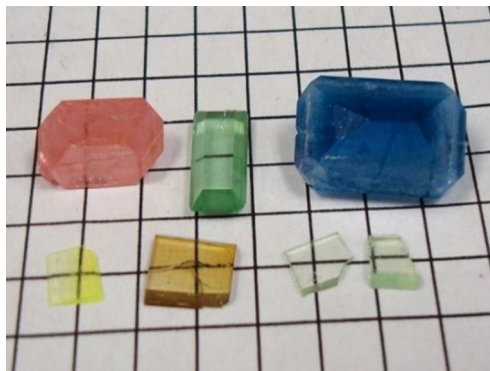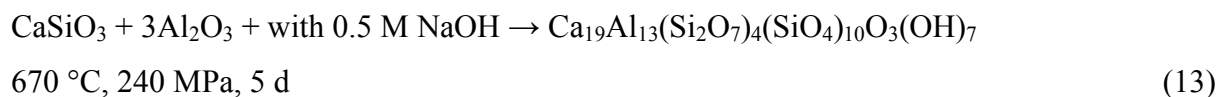
Figure 7: Hydrothermally-grown garnet single crystals (5 mm divisions) based on $Y_3Al_5O_{12}$ (YAG) and $Lu_3Al_5O_{12}$ (LuAG). Top row: Er^{3+}:LuAG, Cr^{3+}:YAG, Yb^{2+},Yb^{3+}:LuAG. Bottom row: Ce^{3+}:LuAG, Ca^{2+},Cr^{4+}:YAG, Pr^{3+}:LuAG (x2).

3.3. Hetero-Oxyanion Silicates

The laboratory hydrothermal results with metal silicates are still in the early stages and only hint at the structural opportunities that await in this field. A simple extension to the aluminosilicates and borosilicates again mimics the most common natural systems and opens many new reaction possibilities. For example, consider the vesuvianite family pictured in Figure 8a. Vesuvianite is a very common mineral found all over the world, but its natural chemistry can only be described as chaotic.[87,88] The nominal formula is $X_{19}Y_{13}Z_{18}T_{0-5}O_{68}W_{10}$ where X = Ca, Na, RE, Pb, Sb; Y = Al, Mg, Fe, Ti, Mn, Cu, Zn; Z = Si; T = B; W = OH, F, O. The material is a beautiful and fascinating structure, but the huge range of substitutional combinations is problematic for properties characterization of natural samples. In fact one paper studied no less than 76 single crystal structures of various substituted vesuvianites in a heroic effort just to understand the structural chemistry of the mineral.[88] To our knowledge, the idealized composition proposed for vesuvianite, $Ca_{19}Al_{11}Mg_2(Si_2O_7)_4(SiO_4)_{10}O(OH)_9$,[88] has not been

thoroughly structurally characterized. Recently however, we prepared a sample of pure prototype crystals from a simplified hydrothermal reaction resulting in an ideal structural arrangement based on the minimum number of unique cations that enables careful structural study.

$$CaSiO_3 + 3Al_2O_3 + \text{with } 0.5 \text{ M NaOH} \rightarrow Ca_{19}Al_{13}(Si_2O_7)_4(SiO_4)_{10}O_3(OH)_7$$

670 °C, 240 MPa, 5 d   (13)

The structure is quite complex, with somewhat of a kaleidoscope design and several channels. With eight- and nine-coordinate Ca sites, and five- and six-coordinate Al sites, this structure again provides extensive opportunities for incorporation of rare earth elements, or substituting certain transition metals into desired coordination environments in a controlled fashion.

As a final case study, we mention the complex borosilicate cappelenite. Natural samples of cappelenite are fairly rare and generally of poor quality. Elemental analysis of a typical natural sample of cappelenite, for example, indicated a composition of $(K_{0.05}Ba_{0.64}La_{0.22}Na_{0.10})(Th_{0.04}Ca_{0.15}Y_{5.74}Ce_{0.09})Si_{2.91}B_{6.07}O_{24}F_2$.[89] After a complicated analysis, the structure of the natural sample could be successfully refined only in space group *P3*, though the authors postulated that an impurity-free sample would exhibit *P6mm* space group symmetry.[90] We found that an ordered pure synthetic analog, $BaEu_6Si_3B_6O_{24}(OH)_2$, was indeed best refined in space group *P6mm*.[91] The structure is noncentrosymmetric and polar due to a concerted orientation of the borate tetrahedra aligned along the c-axis. Thus the material has potential nonlinear optical, piezoelectric, and ferroic properties, and the presence of the dopable rare earth site allows it to act as a host for self-frequency doubling applications. Cappelenite possesses a visually pleasing structure (Figure 8b) with layers of borosilicate rings with sheets of

edge-sharing rare earth clusters alternating along the *c*-axis. The inclusion of boron with the silicate system introduces a new wealth of structural possibilities. Boron can exist in both triangular planar and tetrahedral coordination with oxygen, and like the silicates, can form polymeric species such as chains, rings, and sheets. Given the vast number of silicate structures to build upon, introduction of boron with multiple coordination geometries generates a staggering array of possible metal borosilicate structures. In fact, we often find that a simple borosilicate glass serves as a suitable feedstock for hydrothermal synthesis of borosilicates (reactions 14 and 15). In this way also, the synthetic researcher can tune numerous chemical knobs in a straightforward manner to make new materials inspired from a few mineralogical starting points.
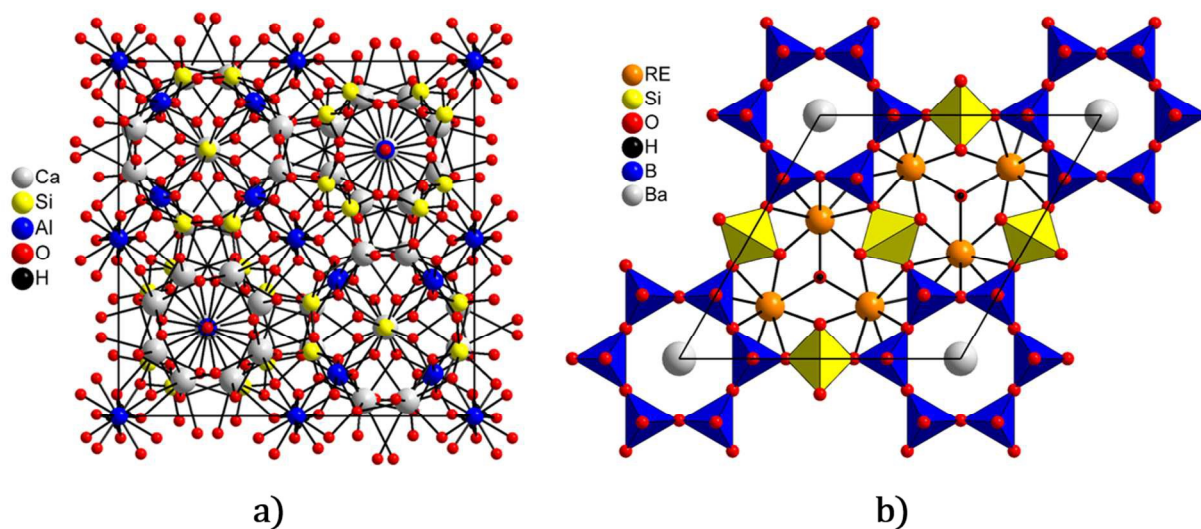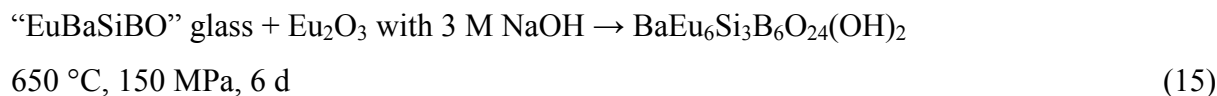
$Eu_2O_3 + 2BaO + 3B_2O_3 + 6SiO_2$ melt $\rightarrow$ "EuBaSiBO" glass

950 °C, air, 18 h   (14)

"EuBaSiBO" glass + Eu_2O_3 with 3 M NaOH $\rightarrow$ $BaEu_6Si_3B_6O_{24}(OH)_2$

650 °C, 150 MPa, 6 d   (15)

a)   b)

Figure 8: Structures of hydrothermally-synthesized simplified mineralogical systems: a) vesuvianite-type $Ca_{19}Al_{13}(Si_2O_7)_4(SiO_4)_{10}O_3(OH)_7$ along [001]; b) cappelenite-type

$BaRE_6Si_3B_6O_{24}(OH)_2$ along [001]. Structural details are: $Ca_{19}Al_{13}(Si_2O_7)_4(SiO_4)_{10}O_3(OH)_7$ in space group *P4/nnc*, with $a = 15.5261(12)$ Å, $c = 11.8047(10)$ Å, Z = 2, and $BaEu_6Si_3B_6O_{24}(OH)_2$ in space group *P6mm* with $a = 10.8074(15)$ Å, $c = 4.7296(9)$ Å, Z = 1.[91]

4. Final Perspectives

In this Perspective, we briefly highlight some of our efforts to use natural mineral crystals as a unifying theme in exploratory solid-state synthesis. By using high temperature hydrothermal methods as our primary synthetic technique, we are achieving approximately similar conditions to those encountered in many natural systems. Hence we observe correspondingly related crystalline products. In our experimental design, we employ the same style of building blocks that works so well in nature, namely mixed combinations of tetrahedra and octahedra. Typically the tetrahedra are classical oxyanion building blocks like silicate, phosphate and vanadate, and they serve as structural directors and linkers. The octahedra are typically created from transition metal ions and these are often open shell species that are responsible for interesting spectroscopy and magnetism. Of course other coordination environments are observed in many cases, but the classical tetrahedral/octahedral combinations are by far the most common and provide an unlimited number of structural options. The reactions are highly tunable and even minor variations in reaction conditions lead to new products. Small modifications can be made to the reactions to introduce rare earth ions as structural building blocks, which opens doors to additional optical functionality.

We can make several broad generalizations about this synthetic approach. Our experimental technique employs temperatures that are at the higher end of the hydrothermal range (ca. 500-700 ˚C) compared to the more heavily investigated regime around 200 ˚C.

Undoubtedly both thermal growth zones also occur commonly in nature. At these higher temperatures we observe a wide range of products that often form crystals of a large size. Typically they do not contain water molecules in the lattice, either coordinated to a metal ion or as a hydration species. This is in contrast to the chemistry observed from low temperature (200˚C) hydrothermal reactions where products containing water molecules are very common. Again we emphasize that both types of solids are observed among the natural mineral types. In contrast to water, the hydroxide molecule is a still an important building block for many types of lattices when the synthesis occurs even as high as 700 ˚C.

It is clear that tetrahedral building blocks are common and versatile, serving as bridges and linkers in many configurations. The d-block and f-block metal ions are all represented. Low dimensionality is common and the overall structures can be tuned by the introduction of both alkali and alkaline earth ions in various stoichiometries. An important factor in any aspect of hydrothermal crystal growth is the character of mineralizers. These are typically small, simple nucleophiles like OH^-, halides or CO_3^{2-} or alternatively, mild protic acids. These are the same mineralizers that are most common in nature and again, this may account for the close similarity in observed products between natural minerals and laboratory crystals. The ability to vary the identity and concentration of the mineralizer provides an important synthetic variable for the growth of new materials.

One important difference between what is observed in the laboratory versus natural minerals is in the purity of the products. Synthetic crystals can be made of essentially complete purity and the identity or concentration of any dopant can generally be carefully controlled, whereas naturally-occurring crystals grow in a much less restricted chemical environment. This can provide a *raison d'etre* for synthetic solid state chemists to pursue intriguing mineral

structures, since synthetic minerals with ideal compositions can serve as a fundamental baseline for understanding the structure and properties of materials.

Terms like "rational design" of solids seem more hopeful than accurate in the hydrothermal laboratory, and we are wary of paying them much heed. We have not yet discerned Nature's materials synthesis strategies with any confidence. Rather our approach is to design experiments that maximize our odds of success, and to look where the light is brightest, namely at classes of compounds that already shine. Identifying an interesting structural feature of a natural mineral, attempting to duplicate its synthesis in the laboratory, and then modifying the reaction to expand the search appears to be an approach with some merit. Take, for example, compounds like reppiaite having an interesting structure and a seemingly random formula of $Mn_5(VO_4)_2(OH)_4$. The fact that such a material can be prepared as large high quality single crystals in high yield suggests that a wide range of other materials also await development in the laboratory. Its occurrence on both a hillside in Italy and in an autoclave in South Carolina, though, perhaps raises more questions than answers.

References

1. F.C. Hawthorne, *Acta Cryst.* 1994, **B50**, 481-510.

2. F.C. Hawthorne, *Am. Miner.* 1985, **70**, 455-473.

3. F.C. Hawthorne, *Can. Mineral.* 1986, **24**, 625-642.

4. P.B. Moore, *Am. Mineral.* 1965, **50**, 2052-2062

5. P.B. Moore, *Science* 1969, **164**, 1063-1064.

6. P.B. Moore, *Am. Mineral.* 1970, **55**, 135-169.

7. P.B. Moore, *N. Jb. Miner Monatsch.* 1970, 163-173,

8. P.B. Moore, *N. Jb. Miner Monatsch.* 1974, **120**, 205-227.

9. R.K. Eby and F.C. Hawthorne, *Acta Cryst.* 1993, **B49,** 28-56.

10. S.R. Krivovichev, *Mineral. Mag.* 2013, **77**, 275-326.

11. E.K.H. Salje, *J. Phys. Condens. Matter* 2015, **27**, 305901.

12. W. Depmeier, *Cryst. Res. Technol.* 2009, **44**, 1122-1130.

13. S.V. Krivovichev (Ed.) *Minerals as Advanced Materials I* Springer-Verlag Berlin Heidelberg 2008.

14. S.V. Krivovichev (Ed.) *Minerals as Advanced Materials II* Springer-Verlag Berlin Heidelberg 2012.

15. A.P. Ramirez, *Ann. Rev. Mater. Sci.* 1994, **24**, 453-480.

16. T. Araki and P.B. Moore, *Am. Mineral.* 1981, **66**, 827-842.

17. P.B. Moore, *Am. Mineral.* 1989, **74**, 918-926.

18. P.J. Dunn, C.A. Francis and J. Innes, *Am. Mineral.* 1988, **73**, 1182-1185.

19. R.M. Hazen, D. Papineau, W. Bleeker, R. T. Downs, J. M. Ferry, T. J. McCoy, D. A. Sverjensky and H. Yang, *Am. Mineral.* 2008, **93**, 1693-1720.

20. F.C. Hawthorne, *Mineral. Mag.* 1998, **62,** 141-164.

21. R.M. Hazen, *Elements* 2010, **6**, 9-12.

22. R. Roy and O.F. Tuttle in *Phys. Chem Earth* L.H. Ahrens, K. Rankama, S.K. Runcorn Eds. 1956, **1**, 138-180.

23. K. Byrappa and M. Yoshimura, Eds. *Handbook of Hydrothermal Technology,* Noyes Publications, Park Ridge, NJ, 2001.

24. S. Somiya Ed. *Hydrothermal Reactions for Materials Science and Engineering,* Elsevier, London, 1989.

25. R.A. Laudise and J.W. Nielson, *Solid State Phys*. 1961, **12** 149.

26. R.A. Laudise, *Prog. Inorg. Chem*. 1962, **3**, 1-47.

27. A. Rabenau, *Angew. Chem. Int. Ed. Engl.* 1985, **24**, 1026

28. C.D. McMillen and J.W. Kolis, *Philos. Mag.* 2012, **92**, 2686-2711.

29. R. Bunsen, *Ann.* 1848, **65**, 70.

30. H. DeSenarmont, *Ann. Chim. Phys.* 1851, **32**, 142-145.

31. C.S. Brown, *Institution of Electrical Engineers,* 1961, Paper #3620 324-327.

32. F. Iwasaki and H. Iwasaki, *J. Cryst. Growth* 2002, **237-239**, 820-827.

33. C.S. McGahey, Ph.D. Thesis, Georgia Institute of Technology, 2009.

34. A.C. Walker and E. Buehler, *Ind. Eng. Chem*. 1950, **42**, 1369-1375.

35. G.W. Morey and P. Niggli, *J. Am. Chem. Soc.* 1913, **35**, 1086-1130.

36. G.W. Morey, *J. Am. Ceram. Soc*. 1953, **36**, 279-285.

37. R.M. Barrer, *Hydrothermal Chemistry of Zeolites,* Academic Press, New York, 1982.

38. S.T. Wilson, B.M. Lok, C.A. Messina, T.R. Cannan and E.M. Flanagan, *J. Am Chem. Soc*. 1982, **104**, 1146-1147.

39. R.A. Laudise, in Crystal Growth of Electronic Materials E. Kaldis (ed.) 1985, Elsevier Science, London, 159-174.

40. T. Gier, *US Pat.* 4 305 778, 1981.

41. R.A. Laudise, W.A. Sunder, R.F. Belt and G. Gashurov, *J. Cryst. Growth* 1990, **102**, 427-433.

42. R.C. Haushalter, K.G. Strohmaier and F.W Lai, *Science* 1989,**246**, 1289-1291.

43. R.C. Haushalter and F.W Lai, *Angew. Chem Int. Ed. Engl.*1989, **28**, 743-746.

44. V. Soghomonian, Q. Chen, R.C. Haushalter, J. Zubieta and C.J. O'Conner, *Science* 1993, **259**, 1596-1599.

45 R.C. Haushalter and L.A. Mundi, *Chem. Mater.* 1992, **4**, 31-48.

46. P.B. Moore and J. Shen, *Nature* 1983, **306**, 356-358.

47. P.B. Moore, *Aust. J. Chem.* 1992, **45**, 1335-1354.

48. J. Cejka, Ed. *Metal-Organic Frameworks Applications from Catalysis to Gas Storage*. 2011, Wiley-VCH, Weinheim Germany.

49. G.C. Kennedy, *Am. J. Sci.* 1950, **248**, 540-564.

50. R.A. Laudise, P.M. Bridenbaugh and T. Iradi, *J. Cryst. Growth* 1994, **140**, 51-56.

51. G.C. Ulmer, H.L. Barnes *Hydrothermal experimental Techniques* John Wiley and Sons 1987, New York.

52. A.N Lobachev Ed. *Crystallization Processes under Hydrothermal Conditions* 1973 Consultants Bureau New York.

53. D.J. Fisher, *Am. Mineral* 1958, **43**, 181-207.

54. M. Schindler, F.C Hawthorne and W.H. Baur, *Can. Mineral.* 2000, **38**, 1443-1456.

55. H.-J. Koo and M.-H. Whangbo, *Inorg. Chem.* 2006, **45**, 4440−4447.

56. A.R. Forbes, C.D. McMillen, H.G. Giesber and J.W. Kolis, *J. Cryst. Growth* 2008, **310**, 4472−4476.

57. M.M. Kimani, C.D. McMillen and J.W. Kolis, *Inorg. Chem.* 2012, **51**, 3588−3596.

58. M.M. Kimani and J.W. Kolis, *J. Lumin.* 2014, **145**, 492−497.

59. M.M. Kimani, H. Chen, C.D. McMillen, J.N. Anker, J.W. Kolis, *J. Solid State Chem.* 2015, **226**, 312-319.

60. L.D. Sanjeewa, M.A. McGuire, V.O. Garlea, L. Hu, G. Chumanov, C.D. McMillen and J.W. Kolis, *Inorg. Chem.* 2015 *54***,** 7014–7020.

61. J.A. Foley, J.M. Hughes and D. Lange, *Can. Mineral.* 1997, **35**, 1027−1033.

62. D.M. Donaldson and W.H. Barnes, *Am. Mineral.* 1995, **40**, 597−613.·

63. L.D. Sanjeewa, V.O. Garlea, M.A. McGuire, C.D. McMillen, H. Cao and J.W. Kolis, manuscript in preparation.

64. M.M. Qurashi and W.H. Barnes, *Am. Mineral.* 1954, **39**, 416-435.

65. L.D. Sanjeewa, C.D. McMillen, D. Willett, G. Chumanov and J.W. Kolis, *J. Solid State Chem.* 2015, in press, doi: 10.1016/j.jssc.2015.07.039.

66. W. Eysel, *Am. Mineral.* 1973, **58**, 736–747.

67. P.B. Moore, *Am. Mineral.* 1973, **58**, 32-42.

68. J.P. Smit, P.C. Stair and K.R. Poeppelmeier, *Chem. Eur. J.* 2006, **12**, 5944-5953.

69. M.M. Kimani, L. Thompson, W. Snider, C.D. McMillen and J.W. Kolis, *Inorg. Chem.* 2012, **51**, 13271-13280.

70. P.B. Moore and T. Araki, *Am. Mineral.* 1972, **57**, 1355-1374

71. A. Möller, N.E. Amuneke, P. Daniel, B; Lorenz, C.R. Cruz, M. Gooch and P.C. W. Chu, *Phys. Rev. B* 2012, **85**, 214422

72. L.D. Sanjeewa, M.A. McGuire, C.D. McMillen, V.O. Garlea, D. Willett, G. Chumanov and J.W. Kolis, manuscript in preparation.

73. J.-H. Liao, D. Guyomard, Y. Piffard and M. Tournoux, *Acta Crystallogr.* 1996, **C52**, 284-286.

74. R. Basso, G. Lucchetti, L. Zefiro and A. Palenzona, *Z. Kristallogr*. 2010, **201**, 223-234.

75. L.D. Sanjeewa, M.A. McGuire, T.M. Smith Pellizzeri, C.D. McMillen, V.O. Garlea, D. Willett, G. Chumanov and J.W. Kolis, manuscript in preparation.

76. J.M. Mann, C.D. McMillen and J.W. Kolis, *Cryst. Growth Des.* 2015, **15**, 2643-2651.

77. E.E. Abbott, M. Mann and J.W. Kolis, *J. Solid State Chem.* 2011, **184**, 1257-1262.

78. M. Pesaro, A.R. Kampfe, C. Ferraris, I.V. Pekov, J. Rakovan and T.J. White, *Eur. J. Mineral.* 2010, **22**, 163-179.

79. C.C. Heyward, M.M. Kimani, C.A. Moore, C.D. McMillen and J.W. Kolis *J. Alloys and Comp.* 2016, 656, 206-212.

80. R. Terry, K. Fulle, L.D. Sanjeewa, C.D. McMillen and J.W. Kolis, manuscript in preparation.

81. G.E. Brown, in *Reviews in Mineralogy*, ed. P.H. Ribbe, Mineralogical Society of America, Chantilly, VA, 5, 1982, p. 275-381.

82. M. Sato, Y. Kono, H, Ueda, K. Uematsu and K. Toda, *Solid State Ionics* 1996, **83**, 249-256.

83. S. Geller, *Z. Kristallogr.* 1967,**125**, 1-47.

84. F.C. Hawthorne, *J. Solid State Chem*. 1981, **37**, 157-164.

85. C.D. McMillen, J.M. Mann, J.Y. Fan. L. Zhu and J.W. Kolis, *J. Cryst. Growth* 2012**, 356**, 58-67.

86. C. Moore, C.D. McMillen and J.W. Kolis, *Cryst. Growth Des.* 2013, **13**, 2298-2306

87. F.M Allen and C.W. Burnham, *Can. Mineral.* 1992, **30**, 1-18,

88. L.A. Groat, F.C. Hawthorne and T.S. Ercit, *Can. Mineral.* 1992, **30**, 19-48.

89. W.C. Brøgger, *Z. Kristallogr. Mineral.* 1890, **16**, 462−467

90. J. Shen and P.B. Moore, *Am. Mineral.* 1984, **69**, 190−195.·

91. C.C. Heyward, C.D. McMillen and J.W. Kolis, *Inorg. Chem.* 2015**, 54**, 905-913.

TOC entry:
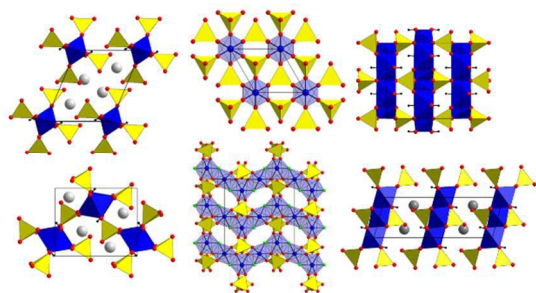
Mineralogically-inspired hydrothermal synthesis provides a wealth of interesting opportunities for the solid-state inorganic chemist.